

## Supporting Information

### Exploring the role of phenothiazine conformations and their interconversion on the electrochemical behaviour of organic electrodes

Yanxiang Gong,<sup>†a</sup> Meng Xia,<sup>†bc</sup> Xiyang Wang,<sup>a</sup> Yunsheng Wang,<sup>ad</sup> Yiran Jia,<sup>bc</sup> Ying Tao,<sup>b</sup> Jun Zhang,<sup>bc</sup> Jie Yang,<sup>a</sup> Manman Fang,<sup>\*a</sup> Quan-Hong Yang,<sup>\*bcd</sup>, Zhen Li<sup>\*adfg</sup> and Ben Zhong Tang<sup>\*e</sup>

<sup>a</sup> *Institute of Molecular Aggregation Science, Tianjin University, Tianjin 300072, China.*

<sup>b</sup> *Nanoyang Group, Tianjin Key Laboratory of Advanced Carbon and Electrochemical Energy Storage, School of Chemical Engineering and Technology, National Industry-Education Integration Platform of Energy Storage and Collaborative Innovation Center of Chemical Science and Engineering (Tianjin), Tianjin University, Tianjin 300354 China.*

<sup>c</sup> *Haihe Laboratory of Sustainable Chemical Transformations, Tianjin, China.*

<sup>d</sup> *Joint School of National University of Singapore and Tianjin University, International Campus of Tianjin University, Binhai New City, Fuzhou 350207, China.*

<sup>e</sup> *School of Science and Engineering, Shenzhen Institute of Aggregate Science and Technology, The Chinese University of Hong Kong, Shenzhen 518172, China.*

<sup>f</sup> *Hubei Key Lab on Organic and Polymeric Opto-Electronic Materials, Department of Chemistry, Wuhan University 430072, Wuhan, China*

<sup>g</sup> *The State Key Laboratory of Luminescent Materials and Devices, South China University of Technology, Guangzhou 510640, China*

\*Corresponding author.

*E-mail:* manmanfang@tju.edu.cn

qhyangcn@tju.edu.cn

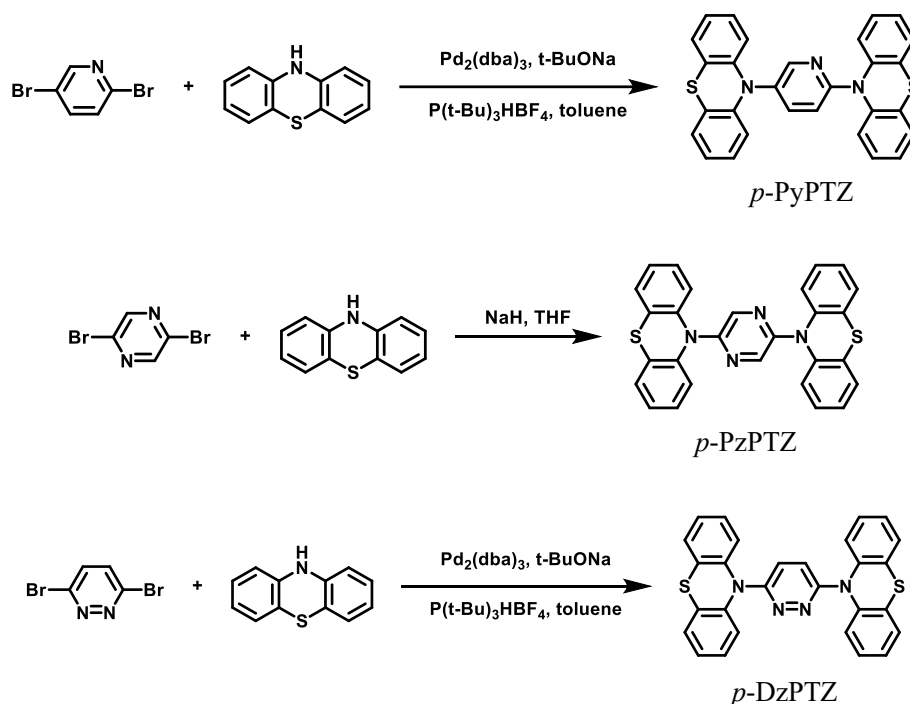
lizhen@whu.edu.cn

tangbenz@cuhk.edu.cn

## Experimental Section

### 1. Synthetic procedure

The target compounds were synthesized according to the previous reports<sup>[1,2]</sup> with some modifications and the NMR data is consistent with the reported data.



**Scheme S1.** Synthetic routes of *p*-PyPTZ, *p*-PzPTZ, and *p*-DzPTZ.

### 2. Materials characterization

$^1\text{H}$  and  $^{13}\text{C}$  NMR spectra were recorded using a 400 MHz Bruker AVANCE III spectrometer. The crystallographic data for *p*-PzPTZ (CCDC No. 2154745) was obtained from the Cambridge Crystallographic Data Centre. Single-crystal X-ray diffraction data (SCXRD) for *p*-PyPTZ and *p*-DzPTZ were collected using an XtaLAB SuperNova X-ray diffractometer. The powder X-ray diffraction (PXRD) patterns were recorded by Rigaku Smartlab9KW. For *ex situ* characterizations, all electrodes were galvanostatically charged and discharged to the corresponding states at 1C, followed

by cell disassembly in an Ar-filled glove box. To remove residual electrolyte, the disassembled electrodes were rinsed three times with DME solution before further analysis. Attenuated total reflection-Fourier transform IR (ATR-FTIR) spectroscopy were obtained on a Nicolet IN10 FT- IR spectrometer. Electron paramagnetic resonance (EPR) spectra were recorded on Bruker EMX plus spectrometer. X-ray photoelectron spectroscopy (XPS) measurements were performed using an ESCALAB 250Xi spectrometer. Field emission scanning electron microscopy (FE-SEM) images were taken by a Regulus 8100 (HITACHI, Japan). *In situ* Raman spectra were recorded with a LabRAM HR spectrometer (Horiba) equipped with a confocal Raman microscope and an argon ion laser excitation source at 532 nm.

### **3. Electrodes preparation**

For the half-cell preparation, the cathode materials were prepared by mixing organic active materials, conductive carbon black (Super P), and poly(vinylidene fluoride) (PVDF) binder at a weight ratio of 5:3:2. The components were then dispersed in an N-methyl-2-pyrrolidone (NMP) solution and stirred for 2 hours at room temperature to form a homogeneous slurry. The resulting slurry was coated onto aluminum foil using a doctor blade technique, followed by dried in a blast drying oven for 8 h and further drying in a vacuum oven at 60 °C for 4 h. The cathodes were then punched into 10 mm diameter circular discs, with the active material mass loading ranging from 0.6 to 1.0 mg cm<sup>-2</sup>.

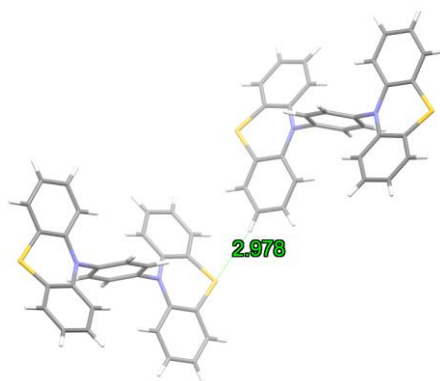
### **4. Electrochemical measurements**

Coin-type CR2032 cells were assembled for electrochemical measurements, utilizing lithium metal as the anode, organic electrodes as the cathode, 20  $\mu\text{L}$  of 1 M  $\text{LiPF}_6$  in EC/DEC (v:v = 1:1) as the electrolyte, and Celgard 2400 polypropylene (PP) membranes as separators. The assembly process was conducted in an argon-filled glove box, with both water and oxygen content maintained below 0.1 ppm. Galvanostatic charge/ discharge measurements were performed using a LAND CT3002AU multichannel battery testing system. Cyclic voltammograms (CV) were recorded using a CH Instruments 660 E electrochemical workstation.

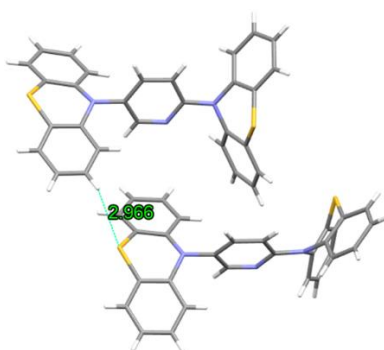
## **5. Calculation**

The Gaussian 09 program was used to perform the time-dependent density functional theory (TD-DFT) calculations. The molecular conformations and single-point energies of neutral molecules and radical cations were optimized at the m062x/6-31g\* level of theory. Additionally, calculations of the lowest unoccupied molecular orbital (LUMO), highest occupied molecular orbital (HOMO), and electrostatic potential (ESP) was conducted.

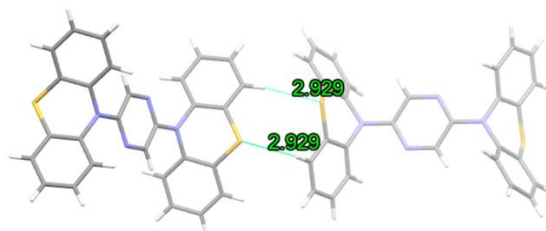
## 6. Experimental data



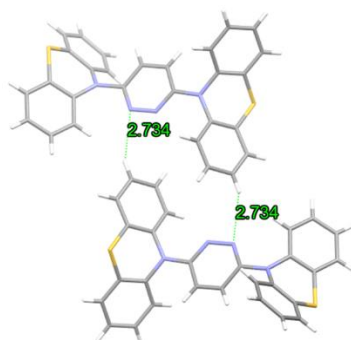
PM-2S: C-H...S 2.978 Å



*p*-PyPTZ: C-H...S 2.966 Å



*p*-PzPTZ: C-H...S 2.929 Å



*p*-DzPTZ: C-H...N 2.734 Å

**Figure S1.** Intermolecular interactions in the single crystal structure of PM-2S, *p*-PyPTZ, *p*-PzPTZ, and *p*-DzPTZ.

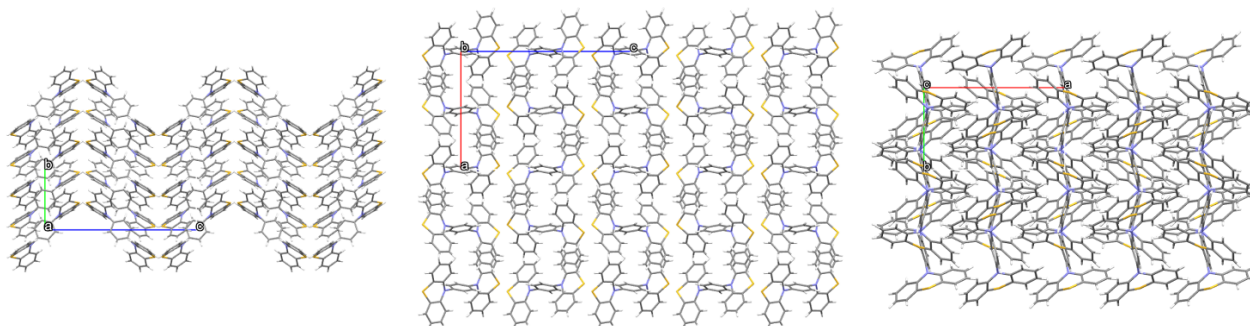


**Figure S2.** Molecular packing in the single crystal structure of PM-2S ( $\rho=1.38 \text{ g/cm}^3$ ).

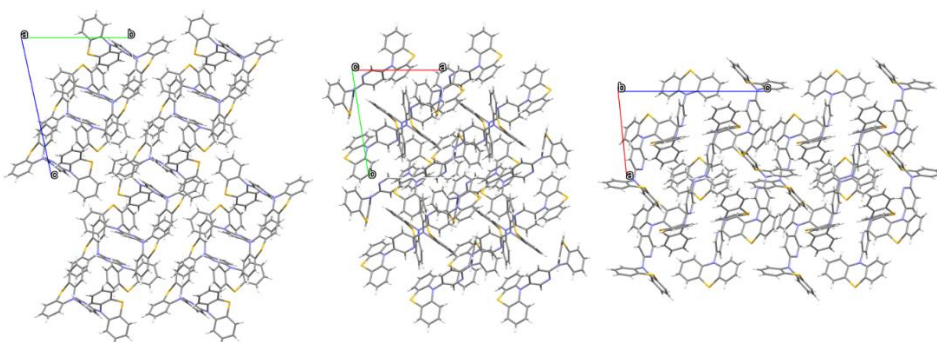


**Figure S3.** Molecular packing in the single crystal structure of *p*-PyPTZ ( $\rho=1.40 \text{ g/cm}^3$ ).

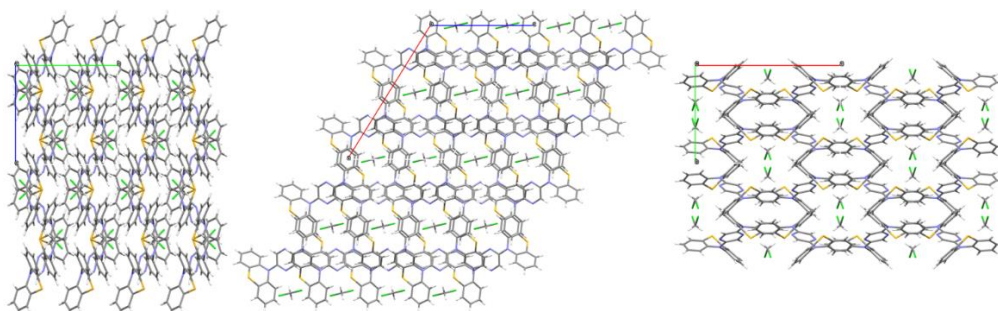


**Figure S4.** Molecular packing in the single crystal structure of *p*-PzPTZ ( $\rho=1.52 \text{ g/cm}^3$ ).

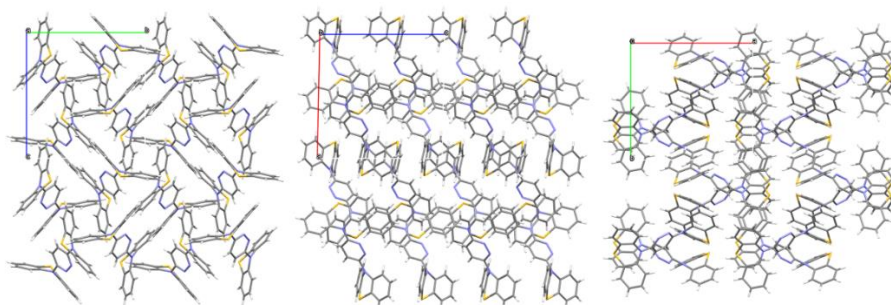


**Figure S5.** Molecular packing in the single crystal structure of *p*-DzPTZ ( $\rho=1.47 \text{ g/cm}^3$ ).



**Figure S6.** Solubility tests of *p*-PyPTZ, *p*-PzPTZ, and *p*-DzPTZ electrodes (from left to right) in the electrolyte.

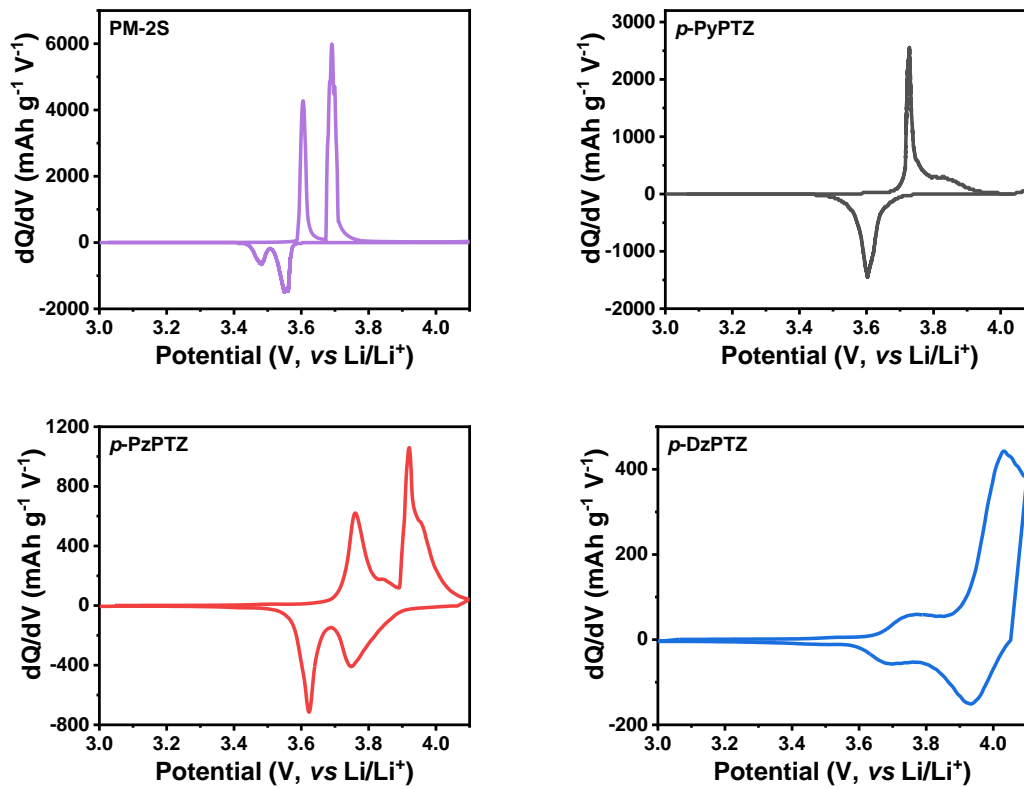


**Figure S7.** The differential capacity ( $dQ/dV$ ) curves of *p*-PyPTZ, *p*-PzPTZ, and *p*-DzPTZ electrodes at 1 C.

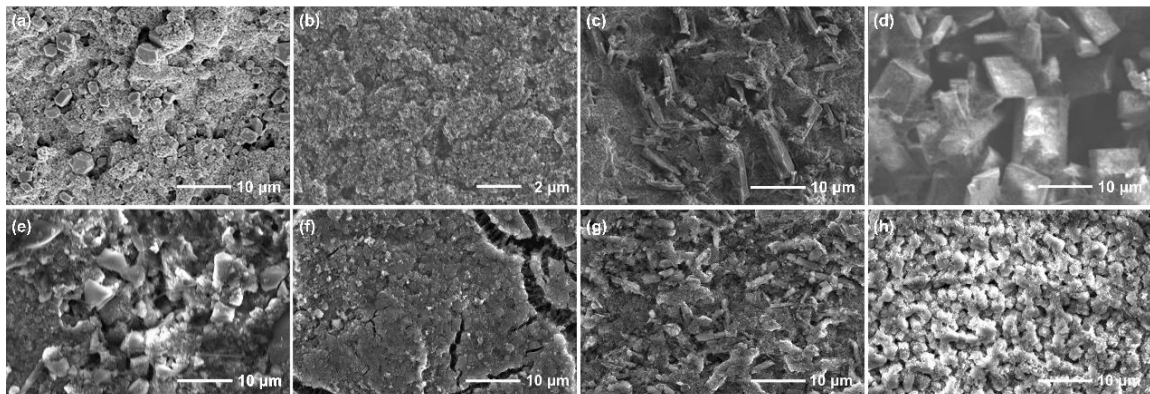


**Figure S8.** SEM images of (a, e) PM-2S, (b, f) *p*-PyPTZ, (c, g) *p*-PzPTZ, and (d, h) *p*-DzPTZ electrodes (a-d) in the pristine states and (e-h) after cycling.

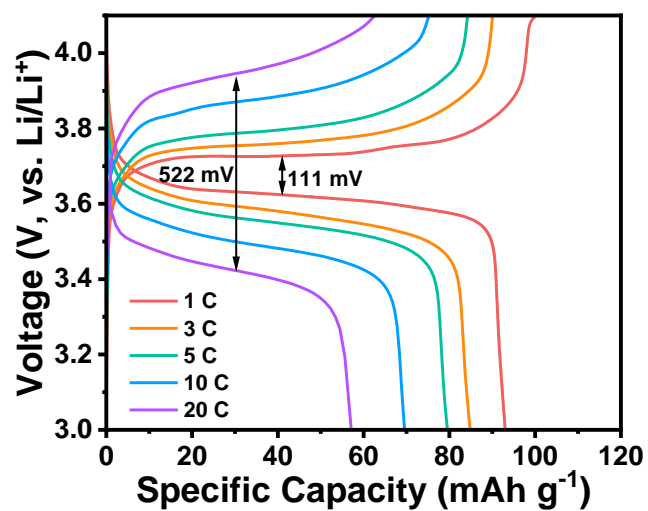


**Figure S9.** Charge/discharge profiles and corresponding charge-discharge plateau voltage difference at different C-rates.

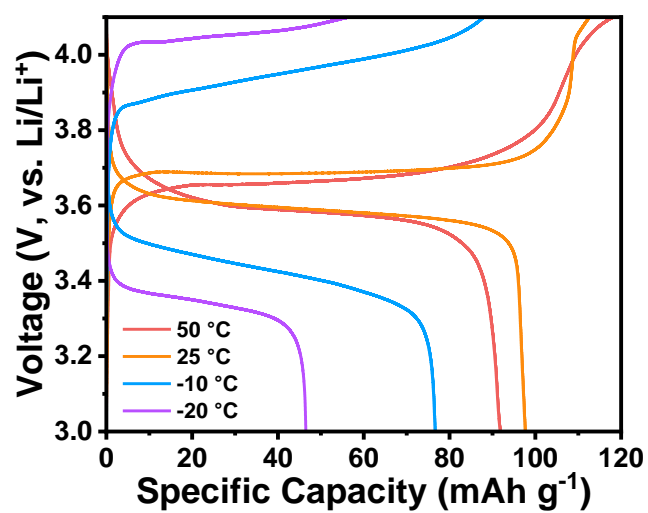


**Figure S10.** Charge/discharge profiles at 1 C at different temperatures.

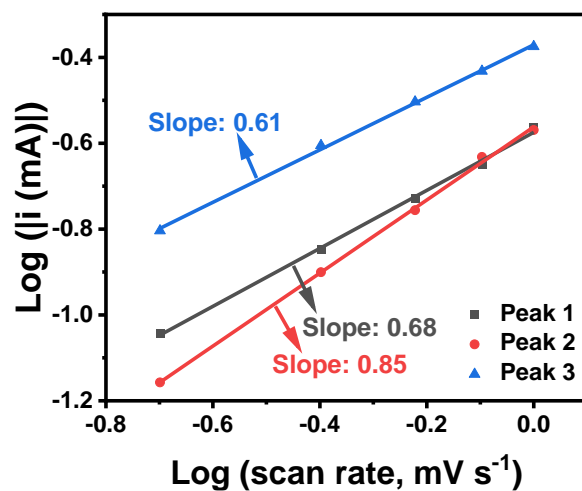


**Figure S11.** The log relationship of peak current and scan rate of PM-2S electrode.

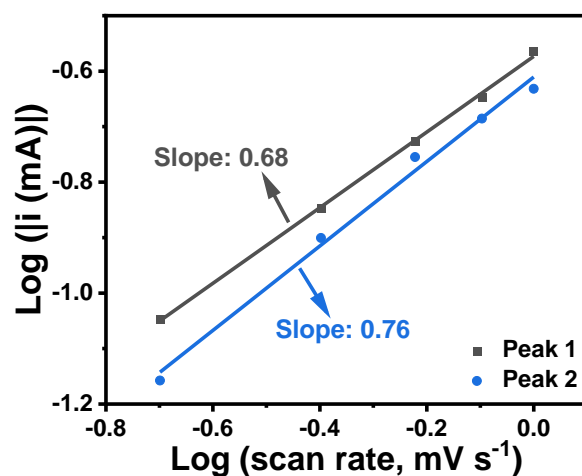


**Figure S12.** The log relationship of peak current and scan rate of *p*-PyPTZ electrode.

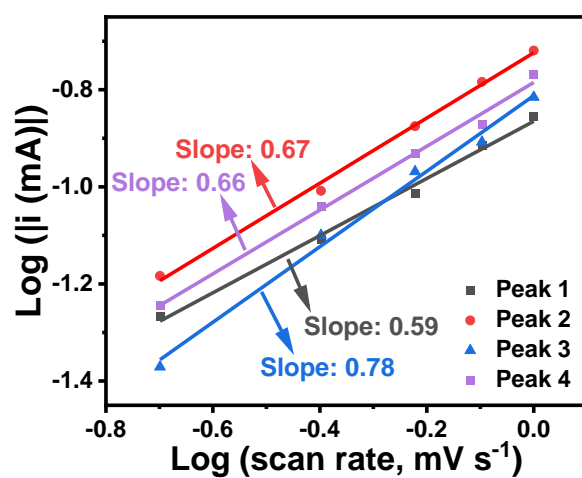


**Figure S13.** The log relationship of peak current and scan rate of *p*-PyPTZ electrode.

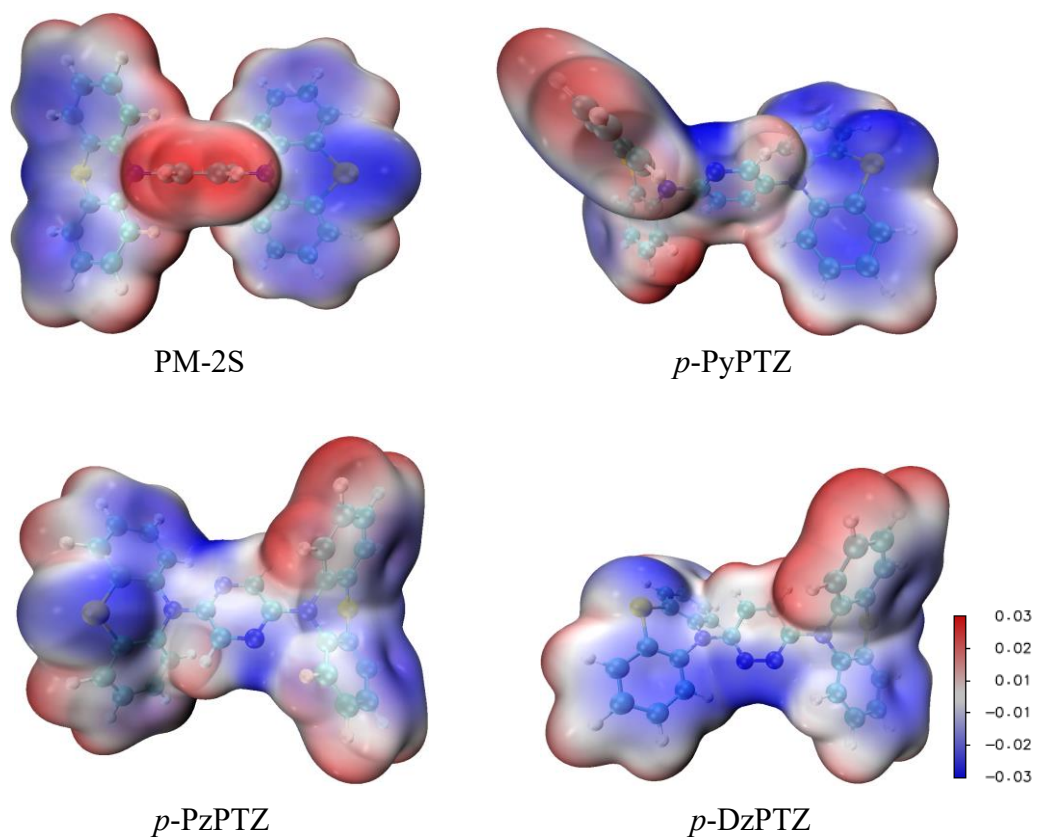


**Figure S14.** The electrostatic potential (ESP) of PM-2S, *p*-PyPTZ, *p*-PzPTZ and *p*-DzPTZ molecules.

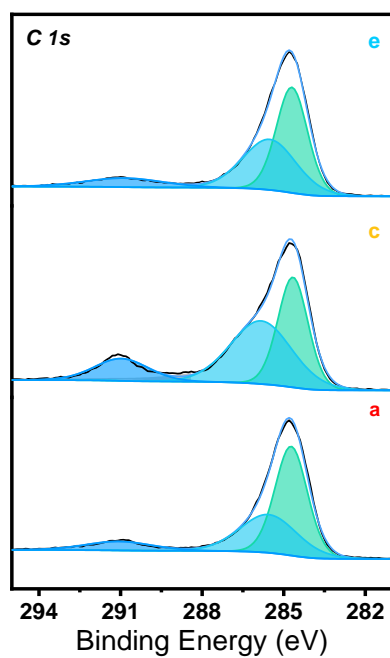


**Figure S15.** *Ex situ* C 1s XPS spectra.

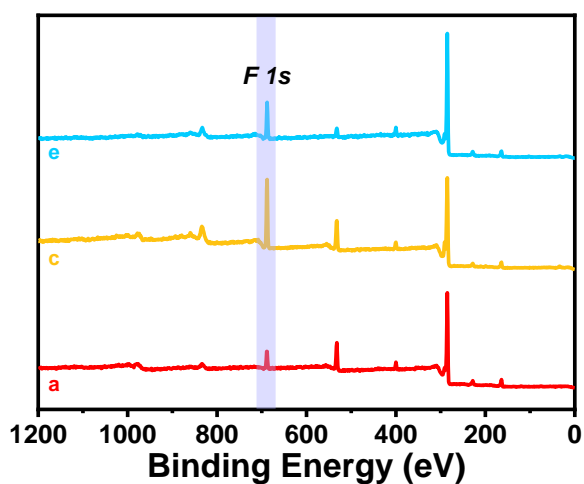


**Figure S16.** The X-ray photoelectron spectroscopy (XPS) full spectrum of *p*-PyPTZ.

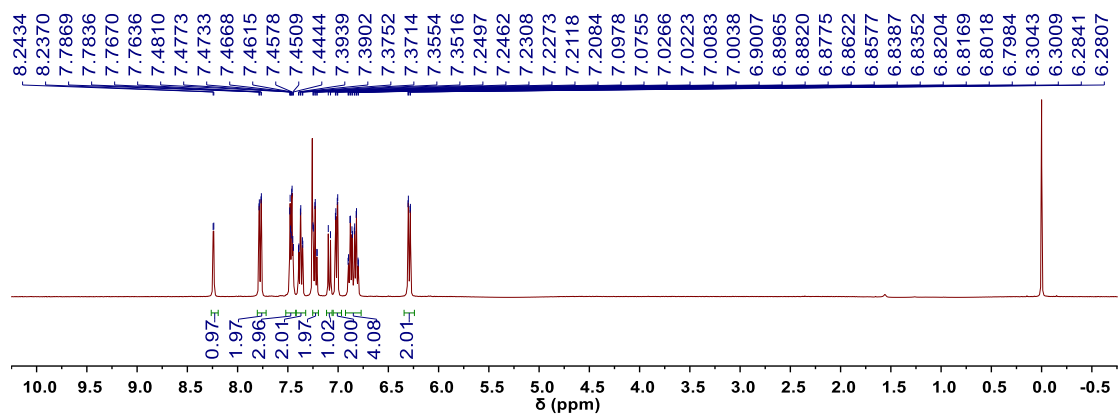


**Figure S17.** <sup>1</sup>H NMR spectrum of *p*-PyPTZ.

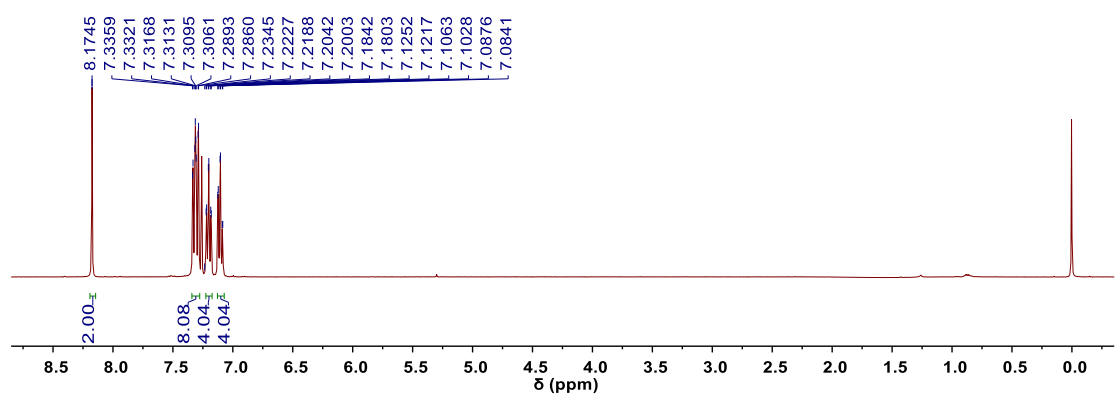


**Figure S18.** <sup>1</sup>H NMR spectrum of *p*-PzPTZ.

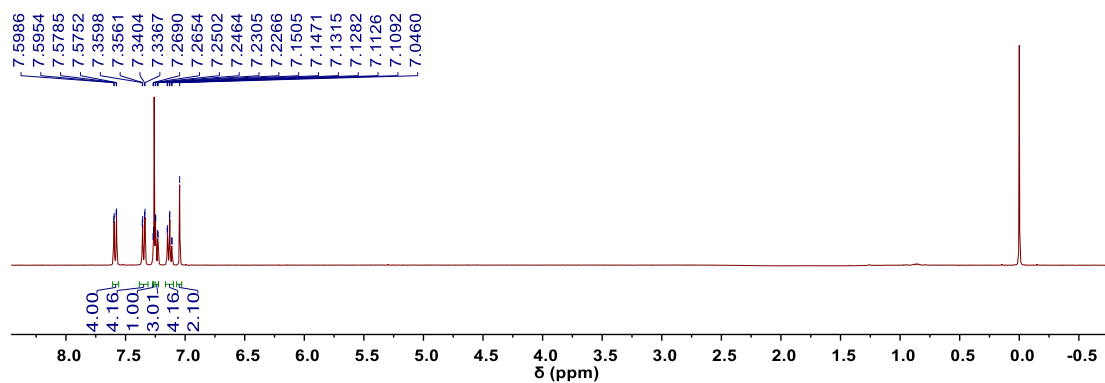


Figure S19.  $^1\text{H}$  NMR spectrum of *p*-DzPTZ.

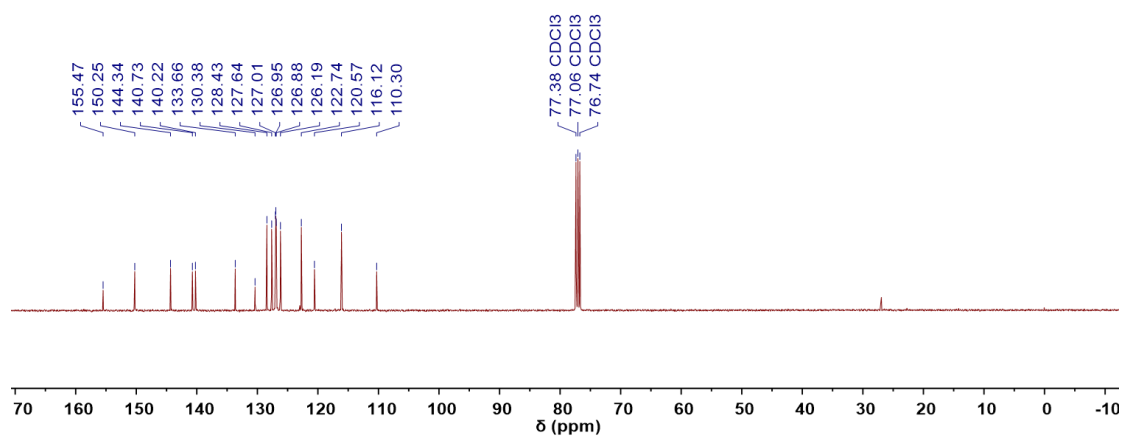


Figure S20.  $^{13}\text{C}$  NMR spectrum of *p*-PyPTZ.

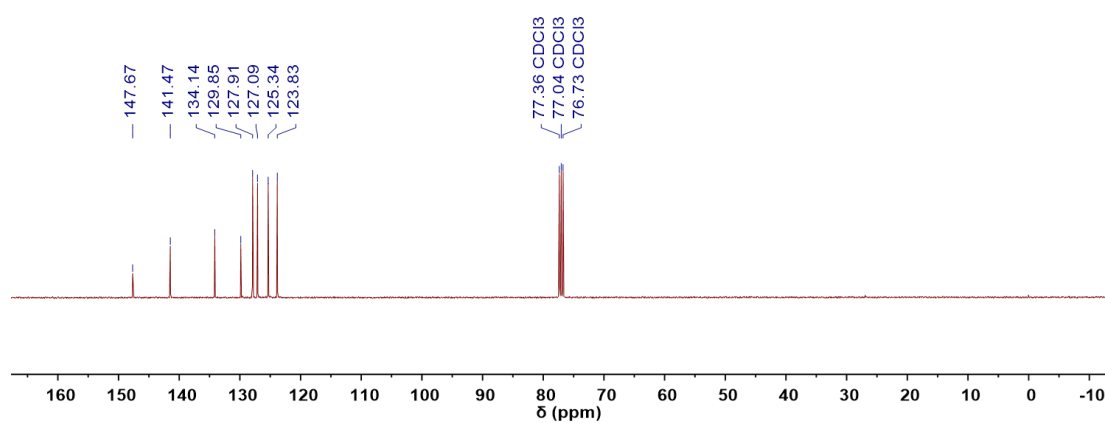
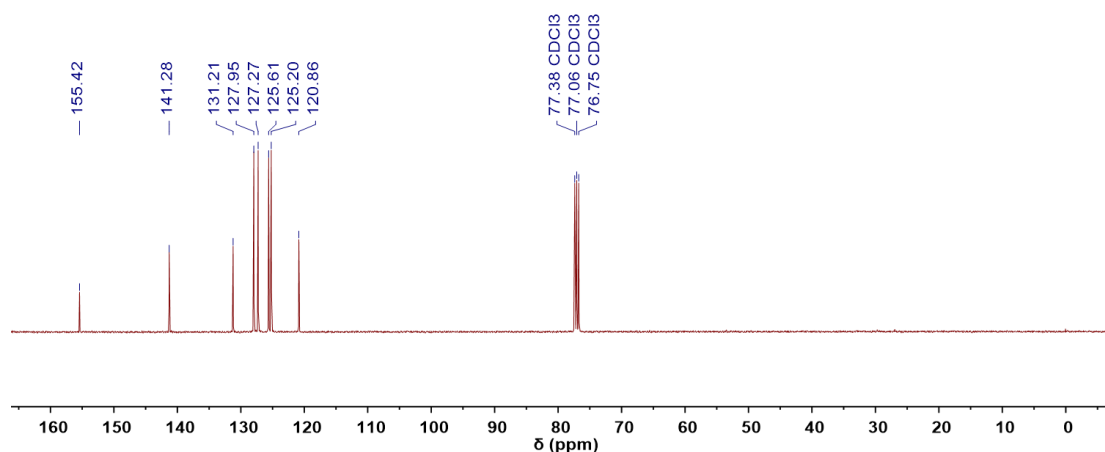


Figure S21.  $^{13}\text{C}$  NMR spectrum of *p*-PzPTZ.



**Figure S22.**  $^{13}\text{C}$  NMR spectrum of *p*-DzPTZ.

**Table S1.** The HOMO energy levels of PM-2S, *p*-PyPTZ, *p*-PzPTZ, and *p*-DzPTZ in different conformations.

		PM-2S	<i>p</i> -PyPTZ	<i>p</i> -PzPTZ	<i>p</i> -DzPTZ
HOMO (eV)	eq-eq	-4.90	-5.15		
	ax-eq	-4.79	-4.97		-4.93
	ax-ax	-4.60	-4.86	-5.03	-5.20

## References

- [1] A. W. Franz, L. N. Popa, F. Rominger and T. J. J. Müller, *Org. Biomol. Chem.*, 2009, **7**, 469-475.
- [2] P. Meti, H. S. Lee and Y. D. Gong, *Dyes Pigment.*, 2022, **204**, 9.